

Spectroscopic and ODMR investigations of the lowest $\pi\pi^*$ and ligand-ligand charge-transfer excited states of zinc(II) mixed-ligand complexes

KAORU NOZAKI¹, SHIGERU IKEDA¹, SEIICHI YAMAMOTO¹,
TAKESHI IKEYAMA^{1†}, TOHRU AZUMI^{1*}, J A BURT² and
G A CROSBY^{2*}

¹Department of Chemistry, Faculty of Science, Tohoku University, Sendai 980, Japan

²Department of Chemistry, Washington State University, Pullman, Washington, 99164-4630
USA

[†]Present address: Department of Chemistry, Miyagi University of Education, Sendai 980
Japan

Abstract. Zero-field splittings of the emitting levels of the title compounds were measured by ODMR. For complexes of the type $Zn(X-PhS)_2(phen)$ resonances of the $^3\pi\pi^*$ phosphorescing levels were observed for $X = F_3, 4-Cl, 4-CH_3$. For $X = 4-Cl$, resonances were detected for the 3LLCT emitting manifold also. For $X = 4-CH_3O$, resonances were detected only for the 3LLCT emitting states. A model invoking mixing between the two types of states is proposed that satisfactorily accounts for the dependences of the properties of the emitting manifolds on the donating ability of the X substituent.

Keywords. Zero-field splittings; Zn(II)-mixed-ligand complexes; LLCT emitting states.

1. Introduction

Excited states of inorganic complexes have captured the attention of spectroscopists and photochemists for several decades. Particularly studied have been ligand-field (LF) excited states in which the excitation takes place mainly on the metal ion leading to substitutional photochemistry in many instances (Balzami and Carassiti 1970). A second class of excited states that has received a great amount of attention is the metal-to-ligand charge-transfer (MLCT) state in which an electron has been promoted from an orbital primarily located on the metal ion to an unfilled orbital primarily located on an attached ligand. The most investigated examples of excited states of this type are those arising in complexes of ruthenium(II) with diimine ligands such as 2,2'-bipyridine and 1,10-phenanthroline (Kalyanasundaram 1982; Juris *et al* 1988). In the MLCT excited state the complexes become both better reductants and better oxidants than in the ground state and thus the opportunity arises for storing excitation energy via appropriately engineered molecular systems, including polymeric materials. Much effort has been expended on ruthenium(II) complexes and its electronic analogs [Os(II), Ir(III), Re(I)] and reports have begun to appear recently in which two metals are connected by bridging ligands. Thus the opportunity arises to design complexes

* For correspondence

such that one metal acts as an antenna for harvesting light and the second center is the locus of subsequent photochemical reactions (MacQueen and Petersen 1990). Photochemical and spectroscopic studies play complementary roles in expanding the frontiers of these areas of research.

In contrast to the substantial effort that has been devoted to the study of both LF and MLCT excited states, relatively few studies have appeared of ligand–ligand charge-transfer (LLCT) excited states of metal complexes. These are complexes in which the absorbed photon transfers an electron essentially from one coordinated ligand (donor) to another ligand (acceptor) complexed to the same metal ion (Crosby *et al* 1985). Although the incidence of such excited states is not rare, complexes in which such LLCT state(s) are the lowest excited states in the molecule have only recently begun to receive attention by spectroscopists and photochemists (Highland *et al* 1986; Yamamoto *et al* 1990). The importance of these types of complexes lies in the fact that radiationless degradation of the excitation energy can be reduced to the point that luminescence from LLCT states can be observed from both low temperature glasses and crystals and thus the properties of the states can be subjected to detailed spectroscopic investigations.

2. Designing complexes

To design a complex that will exhibit low-lying LLCT excited states one generally forms a mixed-ligand complex possessing both a good donor ligand and also a good acceptor. The simplest ones are those with aromatic thiols as the donors and aromatic diimine ligands as acceptors. If, in addition, the purpose is to design a complex that will be luminescent, or potentially luminescent, then an obvious strategy is to use a closed-shell central metal ion such that no low-lying LF states will be present to provide a pathway for efficient degradation of the excitation energy into heat or promote photochemical reactions. Moreover, to prevent any complications arising from the appearance of MLCT transitions in the same region of the spectrum, then a closed-shell metal ion with a high ionization potential is desirable. Thus, Zn(II) and Cd(II) ions become prime candidates for suitable complexes.

3. Current investigations

In the current report we focus attention on a series of zinc complexes of the general formula $\text{Zn}(\text{X-PhS})_2(\text{phen})$ (where X = F, 4-Cl, 4-CH₃, 4-CH₃O; PhS = thiophenol; phen = 1,10-phenanthroline). We also report data on $\text{ZnCl}_2(\text{phen})$ that displays only ligand-localized $\pi\pi^*$ phosphorescence and thus functions in some respects as a standard for comparison. With the single exception of the 4-methoxy derivative all these substances display phosphorescence from both the $^3\pi\pi^*$ and $^3\text{LLCT}$ excited state(s) at sufficiently low temperatures and thus detailed information on both types of states can be obtained. In this current contribution we report data on the zero-field splittings of both $^3\pi\pi^*$ and $^3\text{LLCT}$ excited states as measured by the method of optically detected magnetic resonance (ODMR). We also discuss the origin of the zero-field splitting by means of a proposed state-mixing model that appears to rationalize, satisfactorily, the magnitudes of the observed zero-field transitions.

4. Results

4.1 Luminescence spectra

As a typical example of the luminescence exhibited by these materials we reproduce in figure 1a the spectrum exhibited by $\text{Zn}(4\text{-Cl-PhS})_2(\text{phen})$. The spectrum consists of at least two components – a structured part that has been assigned to the $^3\pi\pi^*$ state of the phen ligand and a broad, diffuse band that maximizes at longer wavelength and is assigned to be LLCT in nature (Highland *et al* 1986). At sufficiently low temperatures (ca. 4 K) each band decays with its own lifetime, ca. 0.5 s for the first peak of the $^3\pi\pi^*$ band and 10–20 ms for the LLCT band. A barrier has been demonstrated to exist between the two states and, by means of heat pulses, the energy stored in the $^3\pi\pi^*$ levels in the crystal can be pumped into the LLCT emissive manifold. The barrier height is of the order of 100 cm^{-1} and is a sensitive function of the nature of the molecule and the structure of the crystal (Highland and Crosby 1985).

Included in figure 1b is the emission spectrum of $\text{Zn}(4\text{-CH}_3\text{O-PhS})_2(\text{phen})$. In contrast to the others, this molecule exhibits only LLCT emission at any temperature. This indicates that no barrier exists in the crystal between excited states of disparate configurations. Also included in the figure is the action spectrum of this complex stimulated by microwave resonance.

4.2 Measurement of zero-field splitting

The ODMR measurements were made on a conventional apparatus. The optical detector was set at a fixed wavelength, the microwave frequency was scanned, and resonances were recorded as variations in the optical signal. The signal was fed to a computer for accumulation and data processing. A schematic representation of the apparatus is shown in figure 2.

4.2a $^3\pi\pi^*$ ODMR: At sufficiently low temperatures, when spin-lattice relaxation is very slow, microwave transitions between spin sublevels can be observed. A typical set is reproduced in figure 3 for the molecule $\text{Zn}(4\text{-Cl-PhS})_2(\text{phen})$.

Transitions occur at 1.54, 2.82 and 4.37 GHz. Since the sum of the first two equals the thirds, we can confidently conclude that these are indeed the transitions between the three sublevels of a triplet term. Similar results have been obtained for other

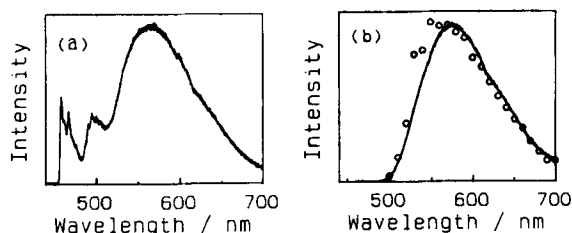


Figure 1. Emission spectra observed from microcrystalline samples at 4.2 K. (a) $\text{Zn}(4\text{-Cl-PhS})_2(\text{phen})$ excited at 380 nm. The structure of the $^3\pi\pi^*$ emission at energies lower than the O–O band is overlapped with vibrational bands of unknown origin that possess a shorter decay time than that of $^3\pi\pi^*$ origin. (b) $\text{Zn}(4\text{-CH}_3\text{O-PhS})_2(\text{phen})$ excited at 380 nm; (o o o) ODMR action spectrum of $\text{Zn}(4\text{-CH}_3\text{O-PhS})_2(\text{phen})$ stimulated at 1.73 GHz.

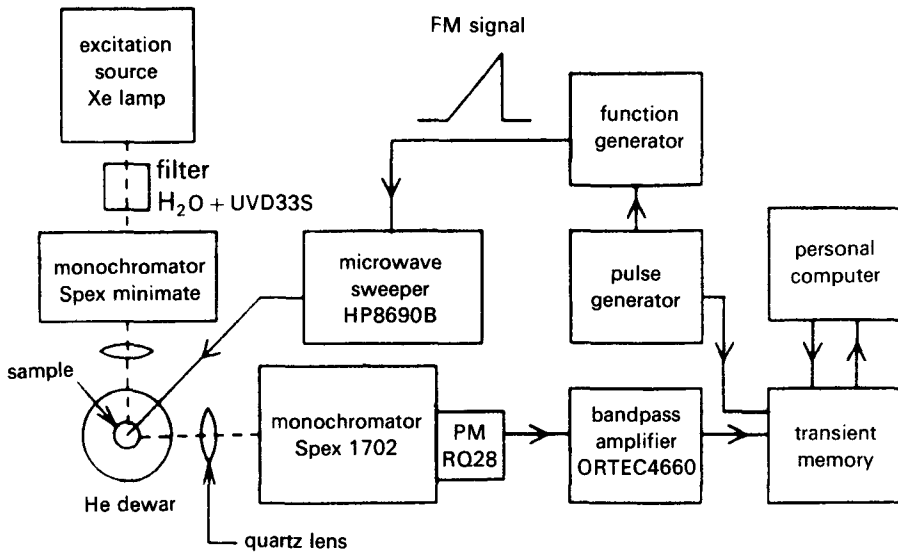


Figure 2. Schematic diagram for measurement of ODMR spectra. ODMR spectra were measured with a Spex 1702 monochromator equipped with a Hamamatsu R928 photomultiplier. Excitation source was 500-W Xe lamp combined with a Spex minimate monochromator and a Toshiba UVD33S glass filter. Microwave power was supplied from a HP8690B sweep oscillator with an appropriate plug-in module. Its frequency was swept in an external FM mode. The signal from the photomultiplier, amplified by an ORTEC 4660 bandpass amplifier, was fed into an Iwatsu DM901 or a Kawasaki Electronica TMR-10 transient memory.

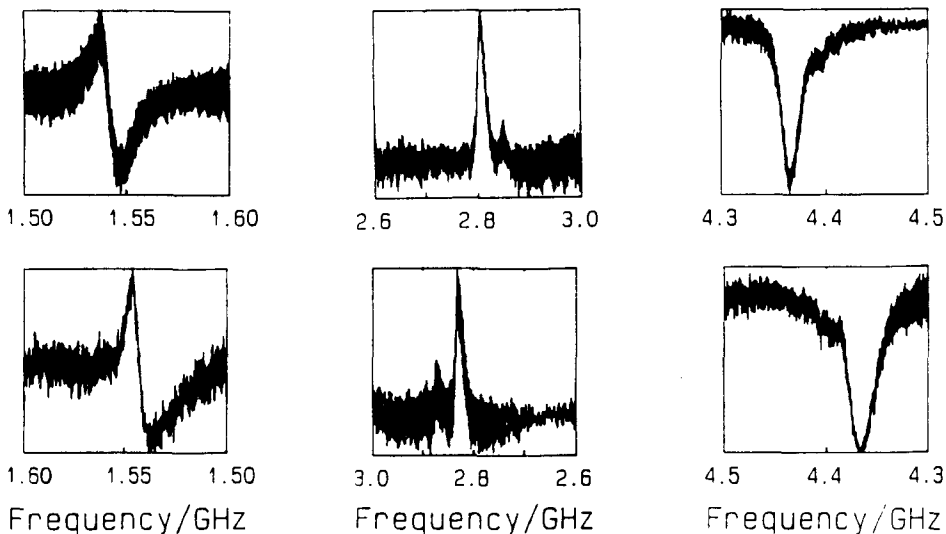


Figure 3. Zero-field splittings of $\text{Zn}(4\text{-Cl-PhS})_2(\text{phen})$ 1:00. Resonances were observed at 1.3 K by ODMR on microcrystalline samples. Since the sweep rate of the microwave generator was not sufficiently slow to prevent distortion of the peak during the scan, the resonant frequency was determined by averaging those measured in both positive and negative directions. All scans in the figure were from left to right.

Table 1. Parameters for the $^3\pi\pi^*$ manifold of Zn(X-PhS)₂(phen) complexes.

	Zero-field transition			D^* (GHz)	k (s ⁻¹)
ZnCl ₂ (phen)	1.55	2.90	4.46	3.92	0.83
Zn(F ₅ -PhS) ₂ (phen)	1.58	2.85	4.42	3.88	1.32
Zn(4-Cl-PhS) ₂ (phen)	1.54	2.82	4.37	3.83	2.08
Zn(4-CH ₃ -PhS) ₂ (phen)	1.46	2.82	4.28	3.76	2.50

Zero-field transitions were measured by ODMR at 1.3 K. Lifetimes were measured at 4.2 K. $D^* = [(3/2)(X^2 + Y^2 + Z^2)]^{1/2}$ where X, Y, and Z are energies of the triplet sublevels measured from their center of gravity.

complexes in the series, and the data are summarized in table 1. We have included the transition energies for ZnCl₂(phen), since this molecule can be considered as an internal standard (*vide infra*). Also listed in the table is the calculated value of D^* for each complex, a convenient parameter for comparing splittings of molecules with such low symmetry (Yamamoto *et al* 1990). In addition we have included the observed decay rate constant of the triplet manifold, measured at 4.2 K.

The complexes in table 1 are listed in order of increasing electron-donating ability of the substituent on the thiol moiety. As the electron-donating ability of the X-substituent increases, all the observed microwave transition energies decrease and D^* also decreases. Further, the decay rate constants of the triplet manifold monotonically increase. The observation that all three microwave transition energies decrease as X varies from pentafluoro- to chloro- to methyl- indicates that the degree of delocalization is increasing. Thus, even though the general features of the phosphorescence spectrum resemble those of the phosphorescence of the uncomplexed phenanthroline ligand, some delocalization occurs over the entire complex even for this so-called 'ligand-localized' $^3\pi\pi^*$ state.

4.2b 3 LLCT ODMR: Although we have attempted to record ODMR signals of the 3 LLCT emitting manifold for all the complexes, we have been completely successful for only one substance, Zn(4-CH₃O-PhS)₂(phen) and partially successful for Zn(4-Cl-PhS)₂(phen). As seen in figure 1b the methoxy complex displays only LLCT phosphorescence. Weak, but reproducible, microwave transitions were observed at three frequencies; 0.28, 1.73 and 2.04 GHz. Again, the sum of the first two almost equals the third and we infer that these are transitions between the three sublevels of the emitting manifold. To corroborate the observations we also measured the ODMR action spectrum, in which the microwave frequency was set at a fixed resonance and the emission monochromator was scanned. Figure 1b demonstrates that the action spectrum closely reproduces the phosphorescence and we can definitely conclude that the three observed microwave transitions are due to transitions among the sublevels of the emitting LLCT triplet manifold.

From the measured 3 LLCT microwave resonances we calculate a value of 1.92 GHz for D^* for Zn(4-CH₃O-PhS)₂(phen). For Zn(4-Cl-PhS)₂(phen) the experimental D^* value is 3.32 GHz. Since we expect a 'pure' 3 LLCT state to have a substantially smaller value of D^* (*vide infra*), the question arises concerning the origin of these unexpectedly large sublevel splittings.

5. Discussion of theoretical models

5.1 $^3\pi\pi^*$ zero-field splitting

To account for the delocalization that is occurring in the ligand-localized $^3\pi\pi^*$ state we have employed a Heitler–London type mixing of the pure $^3\text{LLCT}$ with the pure $^3\pi\pi^*$ state

$$\phi = [\cos \theta] \phi(^3\pi\pi^*) + [\sin \theta] \phi(^3\text{LLCT}). \quad (1)$$

In terms of this mixing, and by neglecting overlap and off-diagonal elements between the ‘pure’ states, we arrive at expressions both for D^* and for the decay rate constant for the emitting triplet state

$$D^* = [\cos^2 \theta] D^*(^3\pi\pi^*) + [\sin^2 \theta] D^*(^3\text{LLCT}), \quad (2)$$

$$k = [\cos^2 \theta] k(^3\pi\pi^*) + [\sin^2 \theta] k(^3\text{LLCT}). \quad (3)$$

To obtain values for the mixing coefficients we approximate the D^* value of the pure $^3\pi\pi^*$ state by assigning to it the observed value for $\text{ZnCl}_2(\text{phen})$, since this molecule possesses no low-lying LLCT state. We have no experimental information for the D^* of a ‘pure’ LLCT state, but we use as a first approximation in (2), a value of 0.65 GHz calculated from a spin-dipole/spin-dipole Hamiltonian (*vide infra*). In a similar manner we approximate the decay constant of the pure $^3\pi\pi^*$ state by inserting the value measured for $\text{ZnCl}_2(\text{phen})$ in (3). The decay constant for the pure $^3\text{LLCT}$ state has been estimated from several experimental studies to be ca. 50 s^{-1} (Yamamoto *et al* 1990).

By use of the approximations described above and the measured values of both D^* and the decay constant for each complex, values of the mixing coefficients have been determined for (2) and (3). They are listed in table 2.

Table 2. $^3\pi\pi^*/^3\text{LLCT}$ mixing coefficients for $\text{Zn}(\text{X}-\text{PhS})_2$ (phen) complexes.

Complex	$^3\pi\pi^*$		$^3\text{LLCT}$	
	$\text{Cos}^2 \theta$	$\text{Sin}^2 \theta$	$\text{Cos}^2 \theta'$	$\text{Sin}^2 \theta'$
$\text{Zn}(\text{F}_5-\text{PhS})_2(\text{phen})$	0.99	0.01		
	0.99	0.01		
$\text{Zn}(4\text{-Cl-PhS})_2(\text{phen})$	0.97	0.03	0.18	0.82
	0.97	0.03		
$\text{Zn}(4\text{-CH}_3\text{-PhS})_2(\text{phen})$	0.95	0.05		
	0.97	0.03		
$\text{Zn}(4\text{-CH}_3\text{O-PhS})_2(\text{phen})$			0.61	0.39

The mixing coefficients for the $^3\pi\pi^*$ levels were evaluated from D^* (top line) and the decay rate k (bottom line). For the $^3\text{LLCT}$ level the mixing coefficients were evaluated from D^* only. For the calculations a computed value of $D^* = 0.65 \text{ GHz}$ and an estimated value of $k = 50 \text{ s}^{-1}$ were assumed for a ‘pure’ $^3\text{LLCT}$ manifold. A value of $D^* = 3.92 \text{ GHz}$ and a rate constant of 0.83 s^{-1} were assumed for a ‘pure’ $^3\pi\pi^*$ manifold.

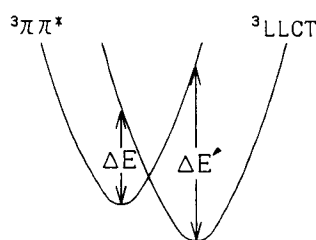


Figure 4. Schematic representation of the potential curves. The magnitude of energy gaps, ΔE and $\Delta E'$, shown in the figure affect the degree of ${}^3\pi\pi^*$ - ${}^3\text{LLCT}$ mixing.

The mixing coefficients determined in the two independent ways are substantially the same. They indicate that the degree of mixing of the LLCT triplet state with the $\pi\pi^*$ emitting triplet manifold increases as the electron donating ability of the X-substituent on the thiol increases. The left-hand side of figure 4 is a pictorial representation of the experimental findings.

As the electron donating capacity of the substituent on the thiol increases, the LLCT state moves to lower energy and the gap, ΔE , between its potential curve and that of the ${}^3\pi\pi^*$ state decreases. This leads to increased mixing of the two states.

5.2 ${}^3\text{LLCT}$ zero-field splitting

We begin by considering, in turn, the possible contributions to the zero-field splittings from spin-spin coupling, spin-orbit coupling, and mixing of the ${}^3\pi\pi^*$ state with the ${}^3\text{LLCT}$ state. We confine our deliberations to the $\text{Zn}(4\text{-CH}_3\text{O-PhS})_2(\text{phen})$ complex, since the geometry is known.

5.2a Spin-spin coupling: To obtain molecular orbitals for the complex for calculation of the spin-spin contribution to the splitting we constructed extended Hückel MOs that were self-consistent with respect to the charge on the central zinc atom (0.57). The excited state geometry was assumed to be the same as that of the ground state as determined by X-ray crystallography (J A Burt and G A Crosby, unpublished work). The resultant HOMO is almost completely localized on the ligating sulfur atoms. The largest HOMO coefficient on any imine atom is only 0.05. The LUMO, however, is virtually restricted to the imine moiety, since the largest LUMO coefficient on any thiol atom is only 0.07. The calculations confirm that the LLCT excited configuration can indeed be viewed as the result of the transfer of an electron from the thiols to the dimine.

With the calculated Hückel orbitals, the spin-dipole/spin-dipole interaction tensor was constructed and diagonalized. The point-charge approximation was employed. The resultant energy levels are $-D_{xx} = 0.42$ GHz, $-D_{yy} = -0.30$ GHz, $-D_{zz} = -0.12$ GHz. These yield a computed value of $D^* = 0.65$ GHz for the LLCT triplet manifold. Although this value is larger than we originally expected, it is still substantially less than the measured value of 1.92 GHz. The reason for the unexpectedly large calculated value for D^* from the spin tensor can be traced to the geometry of the molecule. The crystal structure shows that one of the thiol rings is folded back over the phenanthroline ligand with a face-to-face approach of ca. 400 pm and this leads to the value of 0.65 GHz for D^* . Nonetheless, the calculated spin-spin coupling

cannot account for the measured value of 1.92 for D^* and we search elsewhere for the origin of the unexpectedly large observed splitting.

5.2b Spin-orbit coupling: Since total angular momentum is not a good quantum number in molecules, spin-orbit coupling can only affect the zero-field splitting of triplet manifolds in second order. The expressions for the stabilization of the three spin levels by such interactions are given in standard references (McGlynn *et al* 1969). Each sublevel is affected by three terms, the first two accounting for interactions with higher triplet states and a third that defines the interaction with higher singlet states. Pertinent to the discussion here is the fact that spin-orbit coupling will affect all spin levels equally (isotropic) if the singlet and triplet energies of an interacting configuration are the same.

The Hückel calculations place only LLCT configurations close enough to the lowest LLCT to give non-negligible interactions with it and, furthermore, in the Hückel approximation, the triplet and singlet of a given configuration are degenerate. Thus, any stabilization of the spin sublevels should be isotropic and contribute nothing to the splitting. Moreover, experimentally, we have been unable to measure the $S-T$ energy separation of any LLCT configuration and our supposition is that the singlet and triplet are quasi-degenerate. Finally, we mention the possible contribution of zinc orbitals to the spin-orbit coupling in these types of molecules. Our recent measurements of the series $ZnX_2(\text{phen})$ where $X = \text{Cl, Br, I}$, can be satisfactorily interpreted without invoking any contribution from the zinc $3d$ orbitals (S Ikeda and T Azumi, unpublished work). Thus, both theoretical and experimental evidence point toward a contribution from spin-orbit coupling that is too small to account for the observed zero-field splitting of the emitting ${}^3\text{LLCT}$ manifold, although a definitive answer to the question awaits substantially more sophisticated calculations.

5.2c State mixing with ${}^3\pi\pi^*$: Finally, we appeal to a simple state-mixing model to account for the spin sublevel splitting of the ${}^3\text{LLCT}$ manifold. Such a model satisfactorily accounts for the observed D^* values for the ${}^3\pi\pi^*$ states and it appears reasonable to apply the model here also. Equations (4) and (5), analogous to (1) and (2) above, define the procedure.

$$\psi = [\cos \theta']\psi({}^3\text{LLCT}) + [\sin \theta']\psi({}^3\pi\pi^*), \quad (4)$$

$$D^* = [\cos^2 \theta']D^*({}^3\text{LLCT}) + [\sin^2 \theta']D^*({}^3\pi\pi^*). \quad (5)$$

We assume the calculated value of 0.65 GHz for D^* for the 'pure' LLCT triplet state that was obtained from Hückel theory and the known geometry of the 4-methoxy molecule. This same value is assumed for the 4-chloro complex also. For the pure ${}^3\pi\pi^*$ state we again use the experimental value for the $ZnCl_2(\text{phen})$ complex. Insertion of the measured value of D^* for the $Zn(4\text{-CH}_3\text{O-PhS})_2(\text{phen})$ and $Zn(4\text{-Cl-PhS})_2(\text{phen})$ complex, respectively, yields the desired mixing coefficients. These are included in table 2. Again, the dependence of the degree of mixing on the donating ability of the substituent on the thiol ligand is apparent. The right-hand side of figure 4 depicts the relationship. As the donating ability of the thiol increases, the LLCT potential well shifts downward and the size of the energy gap, $\Delta E'$, increases. Thus, mixing with the ${}^3\pi\pi^*$ state decreases as reflected in the coefficients.

An apparent inconsistency in the model is embedded in table 2 for the

Zn(4-Cl-PhS)₂(phen) complex. The empirically assigned ³LLCT appears to be predominantly ³ $\pi\pi^*$ in character (0.82), a contradiction. Since the complex also shows a barrier between the ³ $\pi\pi^*$ and the ³LLCT emitting states at low temperature, the simple model depicted in figure 4 may not be appropriate in this case. Moreover, the inconsistency may arise from the use of a D^* value for a pure LLCT that is inappropriate for the 4-chloro complex. Nonetheless, the dependence of the mixing on the donating ability of the thiol moiety is retained.

6. Summary and conclusions

Table 2 summarizes the $\pi\pi^*$ -LLCT mixing coefficients determined to date for both the ³ $\pi\pi^*$ and ³LLCT states of these types of metal complexes. For the empirically assigned phenanthroline localized ³ $\pi\pi^*$ state of the complexes in the table the contribution of the 'pure' ³ $\pi\pi^*$ state, as expected, dominates; whereas, for the empirically assigned LLCT emitting state substantial mixing with the ³ $\pi\pi^*$ level is manifest. The table clearly illustrates the main conclusion: A simple ³ $\pi\pi^*$ -³LLCT mixing model accounts for the dependence of these trends in properties of both the ³ $\pi\pi^*$ and ³LLCT states on the electron-donating ability of the thiol ligand.

We have observed the zero-field splittings of both ³ $\pi\pi^*$ and ³LLCT emitting states of a series of metal complexes. The latter observation is the first of its kind. The zinc orbitals do not appear to affect either the splittings or the decay rate constants. A model invoking $\pi\pi^*$ - LLCT mixing satisfactorily accounts for the zero-field splittings of the ligand-localized ³ $\pi\pi^*$ level, the trends in the decay constants of the ³ $\pi\pi^*$ level, and the zero-field splittings of the LLCT level.

Acknowledgements

This research was partially supported by a Grant-in-Aid for International Scientific Research No. 02044011 from the Ministry of Education in Japan. The research was also supported in part by the US Department of Energy under Grant No. DEFD-87ER13809. Such support does not constitute an endorsement of the views expressed in this article.

References

- Balzani V and Carassiti V 1970 *Photochemistry of coordination compounds* (New York: Academic Press)
- Crosby G A, Highland R G and Truesdell K A 1985 *Coord. Chem. Rev.* **64** 41
- Highland R G, Brummer J G and Crosby G A 1986 *J. Phys. Chem.* **90** 1593
- Highland R G and Crosby G A 1985 *Chem. Phys. Lett.* **119** 454
- Juris A, Balzani V, Barigelletti F, Campagna S, Belser P and von Zelewsky A 1988 *Coord. Chem. Rev.* **84** 85
- Kalyanasundaram K 1982 *Coord. Chem. Rev.*, **46** 159
- MacQueen D B and Petersen J D 1990 *Inorg. Chem.* **29** 2313
- McGlynn S P, Azumi T, Kinoshita M 1969 *Molecular spectroscopy of the triplet state* (Englewood Cliffs NJ: Prentice Hall)
- Yamamoto S, Ikeda S, Ikeyama T, Azumi T and Crosby G A 1990 *Chem. Phys. Lett.* **174** 176